Pacek A.W., Chamsart S., Nienow A.W., Bakker A. (1999) The Influence of Impeller Type on Mean Drop Size and Drop Size Distribution in an Agitated Vessel, Chem. Eng. Sci., Oct. 1999, Vol. 54, page 4211-4222.

PERGAMON

Chemical Engineering Science 54 (1999) 4211–4222

Chemical Engineering Science

The influence of impeller type on mean drop size and drop size distribution in an agitated vessel

A.W. Pacek[a,*], S. Chamsart[a], A.W. Nienow[a], A. Bakker[b]

[a]*School of Chemical Engineering, The University of Birmingham, Edgbaston, Birmingham B15 2TT, UK*
[b]*Chemineer Inc., Dayton, Ohio, USA*

Received 7 September 1998; received in revised form 22 February 1999; accepted 9 March 1999

Abstract

In most work on agitated liquid–liquid dispersions, Rushton turbines have been used. Here, mean drop size and drop size distributions are reported for six different impellers covering 3 generic types over a range of mean specific energy dissipation rates. Both viscous and non-viscous dispersed phases have been used at concentrations by volume of 1 and 5%. It has been found that at the same mean specific energy dissipation rate, low power number impellers (whether of the so-called "ultra-high shear" or "high flow" type) all produced similar sized drops at equilibrium which were much smaller than those found with two "high shear", high power number impellers, i.e., the standard Rushton turbine and another six-blade disc impeller. By considering the energy dissipation rate to be confined to the impeller swept volume, these equilibrium drop size could be approximately correlated. The low power number impellers also achieved that equilibrium more rapidly and the drop size distributions in the dispersions produced by them were narrower than those formed when agitated by the Rushton turbine and the other six-blade disc impeller. However, further analysis of the flow in the impeller region and the inclusion of advanced coalescence models would appear to be required in order to enhance the interpretation of these results.

1. Introduction and literature

Hinze (1955) was the first to show, from a balance of the stabilising stress arising from interfacial tension, σ, against the break-up stress due to turbulence in the continuous phase of density, ρ_c, that the maximum stable equilibrium drop size, d_{max}, could be related to the maximum local energy dissipation rate, $(\varepsilon_T)_{max}$, in a stirred vessel by the relationship:

$$(d)_{max} = K_1(\varepsilon_T)_{max}^{-0.4}\left(\frac{\sigma}{\rho_c}\right)^{0.6} \quad (1)$$

Eq. (1) has been shown to apply to experimental data by many workers, for example, Chen and Middleman (1967) and Calabrese et al. (1986). They assumed that $(\varepsilon_T)_{max}$ was proportional to the mean energy dissipation rate, $\bar{\varepsilon}_T$, so that Eq. (1) could be rearranged into the form of the impeller Weber number, *We*. It was also assumed that at equilibrium, $d_{max} \approx d_{32}$, so that Eq. (1) became

$$d_{32}\, D = K_2\, We^{-0.6}, \quad (2)$$

where $We = (\rho_c N^2 D^3\, \sigma)$. D is the impeller diameter and K_1 and K_2 are dimensionless constants.

Davies (1985) modified Eq. (1) to allow for the impact of dispersed phase viscosity as an additional stabilising stress to give an equation of the type

$$\frac{(d_{32})_{u_d}}{(d_{32})_{u_d=0}} = \left[1 + \frac{\mu_d(\varepsilon_T)_{max}^{1/3}(d_{32})_{u_d}^{1/3}}{4\sigma}\right]^{0.6} \quad (3)$$

In Eq. (3), $(d_{32})_{u_d=0}$ is given by Eq. (1) for low-viscosity (inviscid) drops and therefore only accommodates the effect of interfacial tension; and $(d_{32})_{u_d}$ is the drop size for a dispersed phase with the same interfacial tension but of higher viscosity, μ_d. Davies (1985) also used the concept of McManamey (1979) that $(\varepsilon_T)_{max}$ should be based on the assumption that the rate of energy input or power, *P*, given by

$$P = Po\, \rho_c N^3 D^5 \quad (4)$$

was dissipated in the volume swept out by the impeller, V_{imp}, i.e., $(\varepsilon_T)_{max} = (\varepsilon_T)_{imp} = P/\rho_c V_{imp}$. With all these

*Corresponding author. Tel.: 0121-414-5308; fax: 0121-414-5324.
E-mail address: a.w.pacek@bham.ac.uk (A.W. Pacek)

0009-2509/99/$ - see front matter
PII: S0009-2509(99)00156-6

considerations taken into account, Davies (1985) was able to use Eq. (3) as the basis for correlating drop sizes taken from the literature for a wide range of liquid–liquid dispersion devices provided a suitable value for the maximum local ε_T could be estimated for each of them.

In all the above developments, the dispersed phase volume fraction was considered to be sufficiently small that the rate of coalescence was negligible compared to break-up, so that dispersed phase concentration was not included in the equations. With increasing concentration, however, coalescence, especially in the region away from the impeller, was considered to occur; together, possibly with damping of the turbulence in the continuous phase due to the presence of the dispersed phase (Godfrey et al., 1989; Davies, 1992), so that Eq. (2) for inviscid dispersion was empirically modified to give

$$\frac{d_{32}}{D} = K_2(1 + \Phi K_3)We^{-0.6}. \tag{5}$$

Here, as in Eq. (2), K_2, should depend on the impeller type, especially its power number (as indicated by Eq. (4)) and K_3 is a measure of the tendency to coalesce. Systems which coalesce easily, have high values of K_3 and those, which coalesce slowly, have low ones; and regardless of this tendency, as Φ tends to zero, Eq. (5) reverts to Eq. (2). Values for K_3 from about 3 (Godfrey et al., 1989; Davies, 1992) to about 20 (Pacek et al., 1998) have been reported.

Some doubt on the theoretical validity of these equations has recently been mooted by the present workers (Pacek et al., 1998), especially the assumption that d_{32} was only dependent on, i.e., proportional to, d_{max}. Nevertheless, the equations have been found to work quite well by many workers as may be seen from the time scale over which they have been developed and the recent reviews of Davies (1992) and Peters (1997). Therefore, these equations are used here in order to put the present work into the general framework of the literature that is currently available. However, this approach does mean that certain small inconsistencies exist between this study and the earlier one (Pacek et al., 1998) with respect to the data obtained when using Rushton turbines (see also footnote 1).

In fact, most of the experimental work in the literature on liquid–liquid systems has been undertaken with Rushton turbines and whether they or, occasionally, other impellers have been used, generally power data have not been measured. Therefore K_2 values for use in Eqs. (2) and (5) for different impellers are not available. Thus, the concept of $(\varepsilon_T)_{imp}$ as proposed by Davies to enable Eq. (3) to be used for correlating data from different types of dispersing systems has not been tested for different impeller types (though McManamey (1979) used it for different D/T ratio Rushton turbines).

Impeller types have traditionally been characterised only by power numbers, Po and flow numbers, Fl (Oldshue, 1981; Harnby et al., 1997). Only relatively recently have accurate turbulence data been measured and compared for different impellers to give greater insight, e.g., Calabrese and Stoots (1989) and Dyster et al. (1993). It was established many years ago (Cutter, 1966) that the local energy dissipation rate in the impeller region is many times (order 70) higher than elsewhere in a Rushton turbine stirred vessel but values from 10 to 100 have been reported (Nienow, 1998). Because Rushton turbines have high values of Po ($\sim$ 5) compared to Fl ($\sim$ 0.8), the radial flow Rushton turbines have also often been called "high shear impellers", considered especially valuable for gas dispersion and for droplet break-up (Oldshue, 1981). Axial flow propellers and the recently developed hydrofoils such as the Chemineer HE3 which have replaced them have low values of Po ($\sim$ 0.3) and similar values of Fl ($\sim$ 0.6). They have been considered "high flow impellers" especially to be used for bulk blending (Oldshue, 1981), though recent work has suggested that the difference in blending performance between "high shear" and "high flow" impellers at the same mean energy dissipation rate is much smaller than had previously been thought (Nienow, 1997).

In addition to these standard radial and axial flow impellers, other special "ultra-high shear" mixers which in practice typically run at very high rotational speeds, have especially been developed for producing stable, fine liquid–liquid dispersions or emulsions, generally with the addition of surface-active agents. For these, Po and Fl data are rarely available. These latter impellers are often used with very low $D\ T$ ratios and because they are considered to be unable to produce adequate flow (Oldshue, 1981), they may be used in conjunction with another larger $D\ T$ ratio impeller so that the latter ensures good bulk blending. The effectiveness of these "ultra-high shear" impellers as compared to other agitators in terms of the equilibrium drop size as a function of energy dissipation rate or the time to reach equilibrium have rarely been reported.

In this study, two "high shear" impellers, a standard Rushton turbine, RT, and a disc turbine of six blades, 6DT, the latter with each blade deeper and wider than those of the standard Rushton, were compared with the two other impeller types discussed above. The "high flow" impellers were Chemineer High Efficiency HE3 axial flow hydrofoil impellers, HE3L and HE3S (L for large, S for small); and the "ultra-high shear" impellers were also made by Chemineer. These were Chem Shear agitators, Style 2, CS2, and Style 4, CS4, each of the latter being intended for emulsification processes (Fondy and Bates, 1963). The Rushton turbine and three of the four Chemineer impellers (the HE3S and the CS2 and CS4) were of the same diameter ($\sim$ 60 mm); and a special feature of the work was that each of three 60 mm Chemineer agitators had essentially the same Po value ($\sim$ 0.33). Thus, it was possible to compare the

performance of two standard "high shear" impellers with two high efficiency, "high flow" impellers and two "ultra-high shear" mixers. To increase the generality of the findings, two oil phases were used as the dispersed phase, one of viscosity similar to water and one significantly more viscous, each at two dispersed phase concentrations. In each case, water was the continuous phase. The results are reported below.

2. Experimental

2.1. Equipment

The drop sizes in the liquid–liquid dispersions were measured in the experimental rig shown in Fig. 1. Two geometrically similar vessels of diameters 0.150 m (T_{15}) and 0.125 m ($T_{12.5}$) were employed. The data for this paper were mostly obtained from T_{15} but a few experiments conducted in $T_{12.5}$ fitted very well into the general findings and are included here, though they were obtained as part of a separate programme of work. Both vessels were flat bottomed, fitted with a lid so that all air was excluded and the liquid height, H, was equal to the vessel diameter. The vessels had 4 equally spaced stainless-steel baffles, T/10 mm wide, and were placed in a water bath of square cross section made from optically flat glass to avoid distortion and to control temperature to 20°C. Agitation was by any one of the different impellers as discussed above and defined in detail below, placed half way up the height of the vessel. All connections into the vessel were made air tight so that bubble entrainment was totally prevented. Prior to each experiment, the vessel was cleaned very carefully by soaking for several hours with Decon, followed by several rinses with deionised, distilled water.

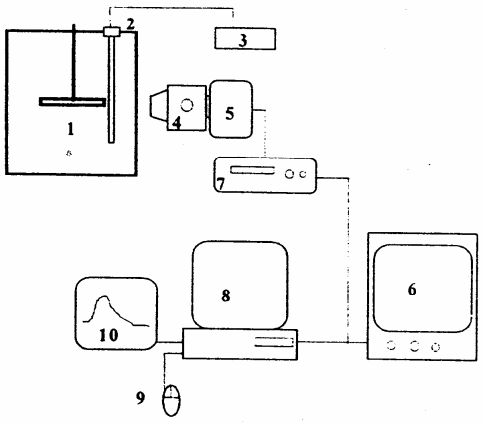

Fig. 1. Experimental rig for the measurement of drop sizes: 1 – stirred vessel, 2 – strobe lamp, 3 – strobe flash, 4 – stereo microscope, 5 – video camera, 6 – TV monitor, 7 – video recorder, 8 – computer with digitizing system, 9 – mouse, 10 – printer.

Mean drop sizes and drop size distributions were obtained by the video–microscope–computer system (Fig. 1) described in detail previously (Pacek et al., 1994). Briefly, a high energy strobe light (2) fed from a strobe flash (3) was placed in the vessel (1) and the gap between the light and the vessel wall could be varied between 2 and 8 mm. A stereo microscope (4) with variable magnification (fitted with an extra lens to give a higher magnification than previously reported) was linked to a video camera (5) with its shutter frequency synchronised to the strobe. Both parameters could be adjusted depending on the agitator speed to produce sharp pictures of drops on the TV monitor (6). The pictures from the video recorder (7) were processed and digitised in the computer (8) and eventually recorded on a laser printer (10). The diameter of the drops in pixels was measured using the mouse (9) to place three points on the drop perimeter. Software converted the data to microns (typically 1–24 μm/pixel) and used geometric binning for data collection. From these data, graphs of frequency (probability density) and cumulative distributions (where the size in the plot is the mean bin size) were calculated, as well as different mean diameters.

Stainless-steel impellers were used, the dimensions of the Rushton turbine and the six-blade turbine being given in Table 1 and Fig. 2; and those of the other

Table 1
Dimensions and Po of the impellers investigated

	Rushton turbine (RT)	Six-blade impeller (6DT)	HE3S	HE3L	CS2	CS4
T (m)	0.125	0.15	0.15		0.15	0.15
D (m)	0.063	0.072	0.063	0.102	0.061	0.060
h (m)	0.012	0.019	0.010[a]	0.016[a]	See Fig 3	
a (m)	0.015	0.024	See Fig. 3			
x (m)	0.002	0.003		See Fig. 3		0.0015
V_{imp} (m^3)	3.75×10^{-5}	7.74×10^{-5}	1.25×10^{-5}	4.90×10^{-5}	7.3×10^{-6}	8.5×10^{-6}
Po	5.0	8.2	0.30		0.32	0.36

[a]Width of impeller blade.

impellers in Table 1 and Fig. 3. Power numbers, Po, for the 6DT, the HE3S, the CS2 and the CS4 were determined from torque measurements using a VISCOMIX torque meter over a wide range of speeds; and that for the Rushton turbine in $T_{12.5}$ was calculated from the correlation published by Bujalski et al. (1987) which has been shown to work well in many other studies at Birmingham since then.

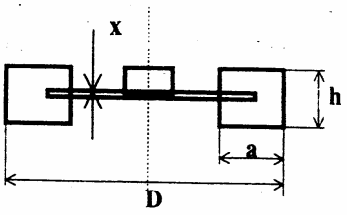

Fig. 2. Rushton turbine and six-blade turbine impeller (see Table 1 for dimensions).

2.2. Materials and methods

The mean drop size and drop size distributions were measured for 1 and 5% by volume organic phases dispersed in water. In all experiments, deionised, distilled water was used as the continuous phase and the organic phase was either chlorobenzene (CLB, $\rho_d = 1106$ kg/m^3, $\mu_d = 0.75$ mPa s, $\sigma = 0.0334$ N/m) as a low viscosity, high density dispersed phase; or sunflower oil (SFO, $\rho_d = 919$ kg/m^3, $\mu_d = 55$ mPa s, $\sigma = 0.027$ N/m) as a viscous, low density dispersed phase. Thus, these two oils

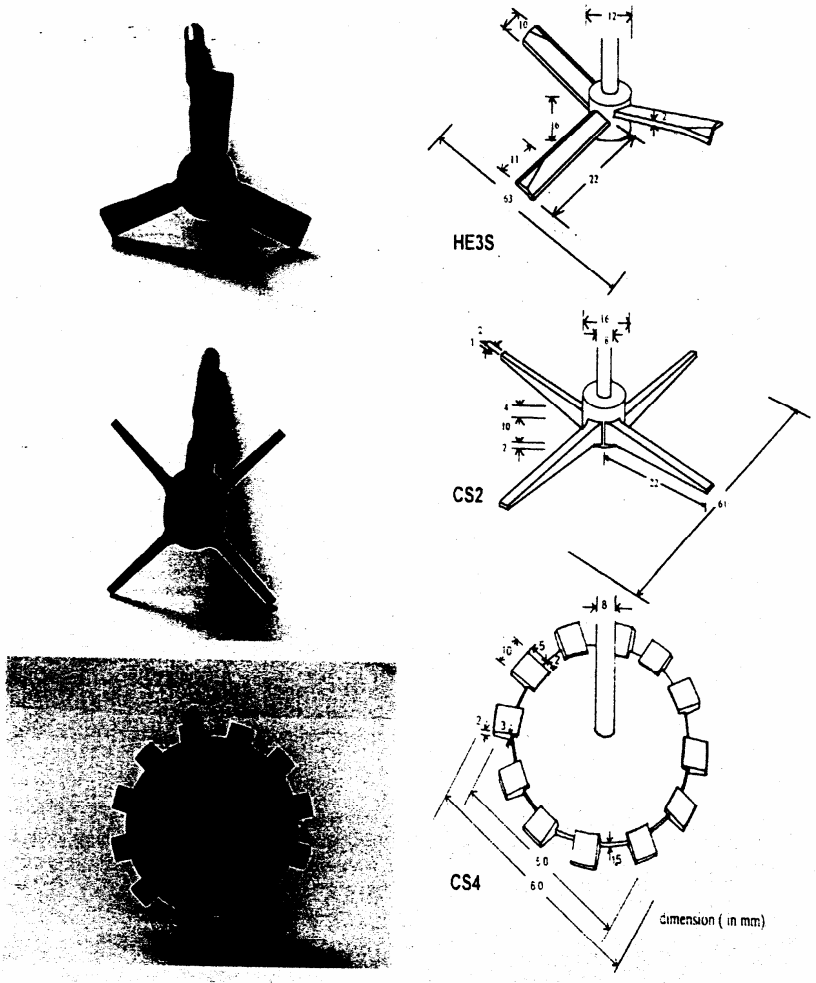

Fig. 3. Dimensions and shapes of ultra-high shear Chem Shear agitators CS2 and CS4 and axial flow hydrofoil impeller, HE3S.

Table 2
System studied (✓) and impeller speeds used

System	RT[a]	6DT	HE3L	HE3S	CS2	CS4
1% CLB		✓	✓			
1% SFO	✓	✓		✓	✓	✓
5% CLB		✓	✓			
5% SFO	✓	✓		✓	✓	✓
Imp speed (rpm)	180.330.480	180.330.480	360.450.540	800.1000.1200	800.1000.1200	800.1000.1200

[a]All experiments were conducted with T_{15} except with the RT.

gave a reasonable spread of physical properties. In addition, whilst SFO was not chemically pure, its use in the manufacture of margarine and low fast spreads gave it a practical importance which compensated for this weakness.

The range of impeller speeds was different for different impellers and the performance of each impeller was investigated at three different speeds (see Table 2). However, there was a considerable overlap in mean specific energy dissipation rates. In all cases, the minimum impeller speed was selected to ensure a visually uniform dispersion in the whole vessel. The stability of the dispersion at this speed was checked by stirring a 5% dispersion for 3 h with careful observation to ensure that separation was not seen. For the 5% SFO water dispersion with small impellers, drop size distributions were measured at two positions in the vessel. One was in the middle and the other near the top since SFO was lighter than water so that if there were any separation, drops should be bigger at the top of the vessel. The results are discussed below. The maximum impeller speed was limited by the quality of images and the resolution of the video technique since the minimum drop size which could be measured accurately was of the order of 10 μm.

The experimental procedure was similar in all cases. The vessel was filled with the required amount of water and oil and great care was taken to remove all air. The system was stirred for 3 h either at the highest or at the lowest impeller speed. After that time, the impeller speed was reduced (or increased) and the drop size distribution was measured every hour up to 3 h. In some experiments with speed increases from zero, measurements were made more frequently to extract drop size transients.

3. Results and discussion

3.1. Power numbers, Po

All power measurements were carried out in the turbulent region and as expected, Po was practically constant for each impeller (see Fig. 4). Also, the three impellers fabricated to have the same Po value were indeed similar: for the HE3S, $Po = 0.30$; for the CS2, $Po = 0.32$; and for the CS4, $Po = 0.36$. These values are in very good agreement with manufacturer's (Chemineer Inc, Dayton, Ohio) data of $Po = 0.33$ for all those impellers, and also with the results reported by Jaworski et al. (1996) for HE3 ($T = 0.102$ m, $Po = 0.305$). Po for the 6DT was 8.2, much higher than Po for a standard Rushton turbine. This increase can be attributed to the much larger area of each blade in comparison with the Rushton turbine as previously shown by Bates et al. (1963). Po for the Rushton turbine was calculated to be 5.0 based on the correlation of Bujalski et al. (1987).

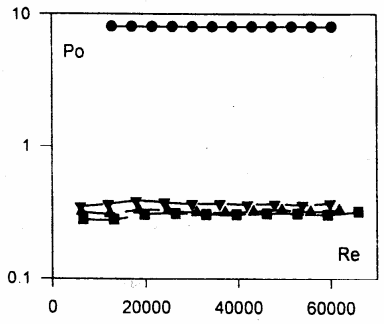

Fig. 4. Power number as a function of Reynolds number for: Six-blade turbine 6DT (●), HE3S (■), CS2 (▲) and CS4 (▼).

3.2. Spatial uniformity of dispersions generated by different impellers

As noted above, the minimum speed for each impeller was selected in such a way that the generated dispersion was visually uniform. Uniformity was checked by measuring the drop size and drop size distributions at different positions in T_{15}, namely at 0.07 and 0.14 m from the bottom. The system chosen was 5% SFO in water using the HE3S, CS2 and CS4 impellers at 800 rpm. The number mean (d_{10}) and Sauter mean diameters (d_{32}) are summarised in Table 3. The results clearly show that the mean drop sizes are independent of the position for all the impellers investigated. The biggest difference between Sauter mean diameters is 10% for the CS4 impeller but this difference is well within experimental error. In addition, the cumulative volume drop size distributions for

each position for the HE3S and CS2 impellers practically overlap (Fig. 5). These mean drop sizes and drop size distributions were measured at the lowest impeller speed and highest volume fraction of dispersed phase, i.e., the conditions which produce the largest drops and therefore the maximum buoyancy force. Clearly, if the means and distributions were independent of position at the lowest speeds used, it can be concluded that at higher impeller speeds with lower volume fractions of dispersed phase and smaller drops, the dispersion would also have been spatially homogenous.

Spatial homogeneity was also reported by Pacek and Nienow (1995) using the system CLB–water agitated by the 6DT in the same T_{15} vessel. CLB in water can be considered a very highly coalescing system since K_3 in Eq. (5)[1] is of the order of 20 or more (Pacek et al., 1998). This value of K_3 is the highest known to the authors.

Table 3
Number mean diameters and Sauter mean diameters at two positions in the 5% SFO dispersion agitated by different impellers at 800 rpm

	d_{10} (μm)		d_{32} (μm)	
Height off the base	0.07 (m)	0.14 (m)	0.07 (m)	0.14 (m)
HE3S	65	70	150	150
CS2	55	60	100	105
CS4	60	70	125	135

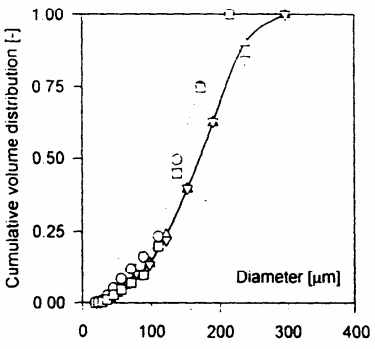

Fig. 5. Cumulative volume distributions for the 5% SFO in water dispersion measured at two heights in the $T = 0.015$ m vessel at $N = 800$ rpm: 0.07 m above the base CS4 (○), HE3S (▽) and 0.14 m above the base CS4 (□), HE3S (△).

[1] In Pacek et al. (1998), it was shown that Eq. (5) is not statistically the best correlating equation for the CLB–water system. However, even allowing a small but statistically significant modification to Eq. (5), the modified equation still clearly showed that CLB–water is a highly coalescing system.

Given these results, it was decided in all other experiments that the drop size distributions should be measured at only one position, i.e., at the mid-height of the vessel.

3.2.1. Comparison with the literature

These present results with SFO–water and our earlier work with CLB–water (Pacek and Nienow, 1995) both show spatial homogeneity. Thus, spatial homogeneity has been demonstrated with two different systems (of which one is highly coalescing) and for a range of agitation conditions. Such results throw considerable doubt on the validity of the conclusions drawn from much earlier and often quoted work by Sprow (1967). He took samples out of the vessel when studying a highly coalescing dispersion of iso-octane in 1% NaCl/water and aimed to freeze the drops by the addition of glycerine before measuring their size by Coulter Counter. When sampling from the impeller discharge stream and from a quiescent region well away from the impeller, he found different mean sizes and different functionalities between drop size and agitator speed for each position. His explanation for the difference was that, in the impeller discharge, break-up controlled the size and in the quiescent region, coalescence. However, given the present results for SFO–water and the other work with CLB–water (Pacek and Nienow, 1995) and considering the relative rates of break-up and coalescence (minutes to hours) compared to recirculation (seconds), it is probable that the difference observed was an artefact of his measurement technique.

3.3. Time required to reach dynamic equilibrium

It has been commonly accepted that after a certain period of agitation of a liquid–liquid dispersion, a dynamic equilibrium between breakage and coalescence is reached and there is no further change in mean drop size or drop size distributions. Typically, for Rushton turbines, these times have been of the order of 2–3 h for low viscosity dispersed phases, e.g., Calabrese et al. (1993) though longer times have also been reported (Lam et al., 1995). Here, too, for the viscous 5% SFO/water dispersion agitated with the Rushton turbine, the drop size distributions continued to change up to 3 h commencing from agitation. After 3 h, the drop size distributions were practically time-independent and a steady state was reached (Fig. 6).

The results obtained with the HE3S, CS2 and CS4 impellers in SFO were very different. In all cases (see Table 4 and two examples also in Fig. 6), the mean size had reached equilibrium in less than 1 h. A comparison of the change of cumulative size distribution as a function of time for the HE3S and RT can be seen in Fig. 7, which again shows that the transient is shorter with the HE3S. Further support is gained from Fig. 8, which shows for

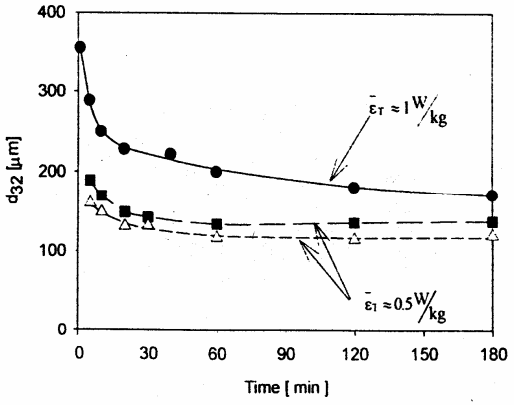

Fig. 6. The d_{32} as a function of time for 5% SFO in water: Rushton turbine (●) at $\bar{\varepsilon}_T \approx 1$ W kg; HE3S (■) and CS4 (△) at $\bar{\varepsilon}_T \approx 0.5$ W kg.

Table 4
Sauter mean diameter in 5% SFO dispersions agitated by different impellers after 1, 2 and 3 h of agitation

Speed (rpm)	d_{32} (μm) HE3S			d_{32} (μm) CS2			d_{32} (μm) CS4		
	1 h	2 h	3 h	1 h	2 h	3 h	1 h	2 h	3 h
800	150	165	145	100	100	105	125	135	140
1000	125	120	120	80	80	85	110	110	110
1200	65	60	65	40	45	45	50	40	50

the CS2 impeller, as an example, that the cumulative size distributions remained practically the same for the period from 1 to 3 h. A similar overlap of drop size distributions was observed with the two other low Po number impellers at 5% dispersed SFO and for all impellers with 1% volume fraction SFO (data not shown).

The shorter time for the HE3 compared to the Rushton turbine is not so surprising if one uses a model (Calabrese, 1997; Smit, 1994) which suggests that the time to reach equilibrium is dependent on how frequently the drops pass through the impeller region. With the simple assumption that

$$t_c = \frac{V}{FlND^3}, \tag{6}$$

where t_c is the circulation time. Since at the same mean specific energy dissipation rate, $\bar{\varepsilon}_T$, for impellers of the same size, from Eq. (4),

$$N \propto Po^{-1/3} \tag{7}$$

then

$$t_c \propto Po^{1/3}/Fl. \tag{8}$$

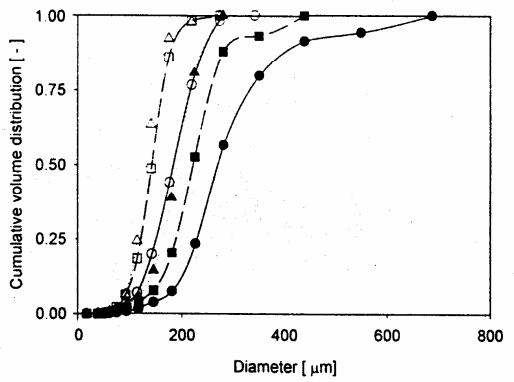

Fig. 7. A comparison of cumulative size distributions for 5% SFO with the Rushton turbine ($\bar{\varepsilon}_T \approx 1$ W/kg) after 5 min (● and solid line), 20 min (■ and dashed line), 180 min (▲ and dotted line) and HE3S ($\bar{\varepsilon}_T \approx 0.5$ W/kg) after 5 min (○ and solid line), 20 min (□ and dashed line) and 60 min (△ and dotted line).

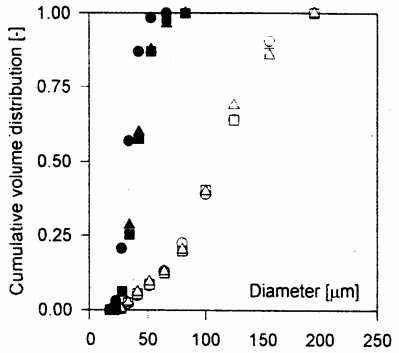

Fig. 8. Cumulative drop size distributions in 5% SFO in water dispersion agitated by CS2 impeller at 800 rpm for 1 h (○), 2 h (□), and 3 h (△) and at 1200 rpm for 1 h (●), 2 h (■) and 3 h (▲).

With the Fl and Po values for the Rushton turbine and the HE3, t_c for the HE3 is about $\frac{1}{2}$ that of the Rushton. Thus, a shorter time of 1–2 h might be expected. However, for the high shear impellers, CS2 and CS4, the flow number is probably very small. For example, for an impeller of this type produced by Ekato (the Sawtooth), Beck (1997,1998) gave $Fl = 0.043$, based on LDA measurements, and $Po = 0.083$. Thus, much longer times might be anticipated from this work and from that of Beck based on the above theory. In fact, as here, very short equilibrium times compared to Rushton turbine impellers were found by Beck (1997,1998) when dispersing 0.13% silicone oil of 1 mPa s in water. It would appear from these results of droplet break-up with ultra-high shear impellers that such a simplistic model cannot explain the very short equilibrium times.

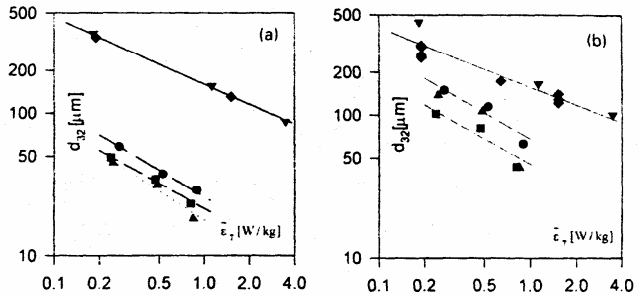

Fig. 9. Steady-state Sauter mean diameters for 1% (a) and 5% (b) SFO in water dispersion agitated by: HE3S (●), CS2 (■), CS4 (▲), RT (◆) and 6DT (▼).

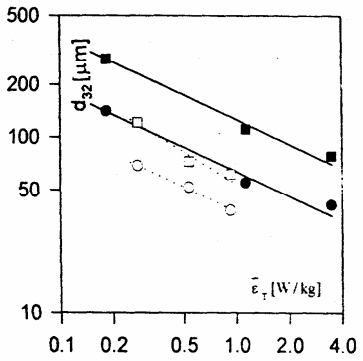

Fig. 10. Steady-state Sauter mean diameters for 1% (○) and 5% (□) CLB in water dispersion agitated by: HE3L (empty symbols) and 6DT (full symbols).

3.4. Drop size and drop size distributions in dispersions agitated by the different impellers

The steady-state Sauter mean diameters for all the impellers investigated for the viscous SFO dispersed phase are shown in Fig. 9 as a function of mean specific energy dissipation rate. At the same $\bar{\varepsilon}_T$, all the low *Po* impellers whether of the "high flow" or the "ultra-high shear" type produced much smaller drops than the Rushton or the six-blade disc turbine. Beck (1997,1998) found very similar trends using the Sawtooth impeller. The difference is more pronounced at the lower volume fraction of dispersed phase (an order of magnitude) than at the higher volume fraction of dispersed phase (drops a few times smaller). Also, as expected, in general, the mean drop sizes are smaller in the lower volume fraction case.

A similar result is found for the CLB using the HE3L and 6DT (Fig. 10). Again the drops with the 6DT are h greater than with the HE3L. Also, in passing, it can ɔeen that the drops of the more viscous SFO are greater than with CLB at equal $\bar{\varepsilon}_T$ values and the same agitator, e.g., with the 6DT at 1 W/kg, $d_{32} = 75$ and 120 μm with 1 and 5% CLB respectively (Fig. 10) but 180 and 200 μm respectively in the SFO (Fig. 9). Thus, these results support the concept that a higher viscosity dispersed phase stabilises the drops and increases their size (Davies, 1985; Calabrese et al., 1986).

Table 5
Exponent *b* in Eq. (9) for different impellers and fluids

Impeller type	1% SFO *b*	5% SFO *b*	1% CLB *b*	5% CLB *b*
Rushton and six-blade turbine	−0.47	−0.41	−0.47	−0.47
HE3S	−0.63	−0.61	—	—
HE3L	—	—	−0.47	−0.62
CS2	−0.59	−0.59	—	—
CS4	−0.68	−0.72	—	—

The Sauter mean diameters have also been correlated with mean specific energy dissipation rate as

$$d_{32} \propto (\bar{\varepsilon}_T)^b \tag{9}$$

and the values of *b* are given in Table 5. Obviously the values of *b* shown in Table 5 should be treated rather carefully since each value is from the regression of the only 3 experimental points. However, there seems to be a certain trend emerging. The exponent *b* for the Rushton and the 6DT are fairly close to the theoretical value of −0.4 (0.41–0.47) as indicated in Eq. (1) (and within the range reported earlier by Pacek et al. (1998)). However, for the low *Po* impellers in all but one case (1% CLB), much lower values of *b* between −0.72 and −0.59 were obtained. Regardless of impeller type, the physical phenomena opposing break-up are the same for each fluid pair, i.e., interfacial tension for the CLB–water and interfacial tension and viscosity for SFO–water. Thus, as the exponents change as the impeller type changes, it suggests that low *Po* impellers may cause break-up by mechanism (s) different from those found with high *Po* impellers. This possibility is discussed further below.

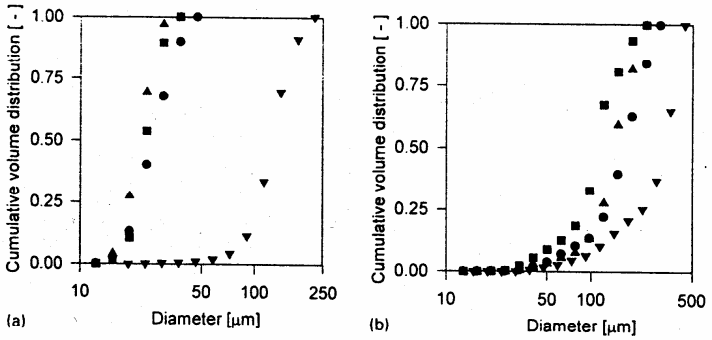

Fig. 11. Cumulative volume distributions: (a) 1% SFO in water dispersion: HE3S, $\bar{\varepsilon}_T = 0.90$ (●); CS2, $\bar{\varepsilon}_T = 0.82$ (■); CS4, $\bar{\varepsilon}_T = 0.85$ (▲); RT, $\bar{\varepsilon}_T = 1.52$ (▼); (b) 5% SFO in water dispersion: HE3S, $\bar{\varepsilon}_T = 0.27$ (●); CS2, $\bar{\varepsilon}_T = 0.24$ (■); CS4, $\bar{\varepsilon}_T = 0.25$ (▲); RT, $\bar{\varepsilon}_T = 0.20$ (▼).

A difference in breakage mechanisms may also be the reason for the different character of the cumulative volume distributions of which examples are shown in Fig. 11a and b. In this figure, the cumulative volume distribution in 1 and 5% SFO dispersions at similar mean specific energy dissipation rates are compared using data taken from experiments with each of the HE3S, CS2, CS4 and RT. These distributions again clearly show that the RT produces much larger drops (even in Fig. 11a where $\bar{\varepsilon}_T$ for the Rushton is 60% higher than with the other impellers). However, plotted this way, it can also be seen that both for the 1 and 5% dispersion, the cumulative volume distributions are much wider for the Rushton turbine than for the other impellers. Based on the bin sizes used to cover the full distribution for each case shown in Fig. 11, in the 1% dispersion, the low *Po* impellers give $d_{max}/d_{min} \approx 4$ (with $d_{min} \simeq 12$ μm) whereas for the Rushton turbine, $d_{max}/d_{min} \approx 12$ ($d_{min} \simeq 20$ μm); in the 5% dispersion, the equivalent values are ≈ 12 ($d_{min} \simeq 20$ μm) and ≈ 15 ($d_{min} \simeq 30$ μm) respectively. This difference in the width of the distributions implies that low *Po* impeller may be particularly attractive in processes where both a small and a more uniform drop size is desired.

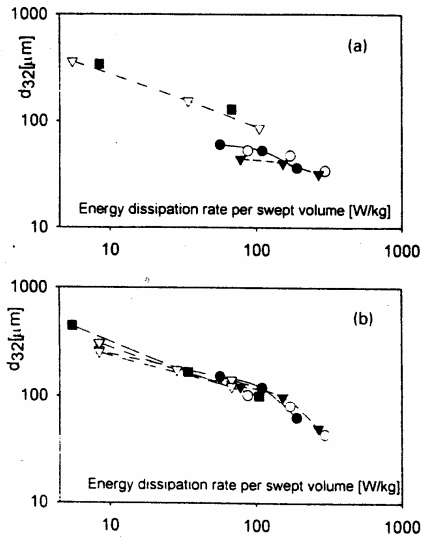

Fig. 12. Sauter mean diameter as a function of energy dissipation rate per impeller swept volume for 1% (a) and 5% (b) SFO in water dispersions agitated by different impellers: HE3S (●), CS2 (○), CS4 (▼), 6DT (▽), RT (■).

3.5. Further comparison with the literature

3.5.1. The basis for the energy dissipation rate for correlating the data

It is interesting to see whether the much smaller drops associated with the low *Po* impellers can be explained by the concept of McManamey (1979) and Davies (1985), namely that the drop size should be correlated by assuming that all of the power input is dissipated in the swept volume of the impeller, i.e., $(\varepsilon_T)_{imp}$ is used as an estimate of $(\varepsilon_T)_{max}$. With this concept, $(\varepsilon_T)_{max}$ is greatly increased, especially for the low *Po* impellers. Fig. 12 shows the modified data for the 1 and 5% SFO based on V_{imp} values given in Table 1. Whilst this approach seems to work quite well at 5%, it is not so good at 1%. Since at 5%, significant coalescence might be expected so that the model should be less applicable, it is concluded that this simple model is not entirely satisfactory with these systems. On the other hand, this procedure is significantly better than using $\bar{\varepsilon}_T$ and perhaps if measured local energy dissipation rates were used to obtain $(\varepsilon_T)_{max}$, it would work well.

3.5.2. Steady-state values with Rushton turbines

It is interesting to compare the data obtained with the Rushton turbine with the equation given by

Table 6
Comparison with correlation of Calabrese et al. (1986) for Rushton turbine impeller for SFO in water

N (rpm)	Experimental d_{32}		Calculated d_{32}	
	$\Phi = 0.01$	$\Phi = 0.05$	$\Phi = 0.01$	$\Phi = 0.05$
240	180	280	210	230
360	–	175	135	150
480	110	130	105	110

Calabrese et al. (1986):

$$d_{32}/D = 0.054(1 + 3\Phi)We^{-0.6}\left[1 + 4.42Vi(1 - 2.5\Phi) \times \left(\frac{d_{32}}{D}\right)^{0.33}\right]^{0.6}. \quad (10)$$

The comparison with the present SFO results is made in Table 6. As can be seen, quite good agreement is obtained at lower volume fraction of dispersed phase but at higher volume fraction, Eq. (10) underpredicts the Sauter mean diameter. However, perhaps this is not surprising since Eq. (10) was meant to apply only to systems in which the larger size arose because the dispersed phase damped the turbulence and not when coalescence occurred.

3.5.3. The relationship between d_{32} and mean specific energy dissipation rate

Eq. (1) applies only to low concentration dispersion for which coalescence can be neglected. The exponent -0.4 on $(\varepsilon_T)_{max}$ comes from estimating the break-up stresses from Kolmogoroff's theory of isotropic turbulence and assuming that the critical turbulent eddy size for break-up is of the order of the maximum stable drop size. If, however, it is assumed that it is the turbulent Reynolds stresses (for example, $\rho_c\overline{u'v'}$) in the impeller region that cause break-up and that the stabilising stress is σ/d, then the maximum stable drop size will be given by

$$\sigma/d_{max} \propto \rho_c\overline{u'v'}. \quad (11)$$

It is well known that the radial rms fluctuating component, $\sqrt{\overline{u'^2}}$, in the discharge stream from the impeller at turbulent Re numbers is proportional to the tip speed (e.g., Dyster et al., 1993), i.e.,

$$\sqrt{\overline{u'^2}} \propto \pi ND. \quad (12)$$

Therefore, though the Reynolds shear stresses are not readily available, if it is assumed that $\sqrt{\overline{v'^2}}$ is also proportional to the tip speed, then it implies that

$$\overline{u'v'} = R_{uv}\sqrt{\overline{u'^2}}\sqrt{\overline{v'^2}} \propto N^2D^2. \quad (13)$$

Thus, it follows that for this model

$$d_{max} \propto \sigma/\rho_c N^2D^2 \quad (14)$$

or

$$d_{max}/D \propto (We)^{-1}. \quad (15)$$

Alternatively, this can be expressed as

$$d_{max} \propto N^{-2} \quad (16)$$

and since $\bar{\varepsilon}_T \propto N^3$, it follows that in this case

$$d_{max} \propto (\bar{\varepsilon}_T)^{-0.67}, \quad (17)$$

i.e., a functionality similar to the range of experimental b values found for all the low Po impellers. It seems possible that the very characteristic trailing vortex structure of the Rushton and other flat blade disc turbines (Nienow, 1998) may lead to break-up occurring differently when compared to other impellers.

It is perhaps surprising that the slopes i.e., b values in Table 5 (and therefore perhaps conceptually the mechanism of break-up) with the HE3 "high flow" impellers should match those of the "ultra-high shear" impellers. It is however worth observing that perhaps very close agreement with Hinze–Kolmogoroff's theory itself should not be expected. After all, it is meant to apply in highly turbulent, homogeneous isotropic turbulence. Break-up clearly occurs in the impeller region and yet in this region, the flow is neither isotropic nor homogeneous (see, for example, Rutherford et al., 1996). It would appear that working with impellers other than Rushton turbines, which has rarely been done in depth in the past, is indicating weaknesses in detail (as has other recent work (Pacek et al., 1998)) in the Hinze Kolmogoroff approach, even though the theory does appear to give some valuable insight into breakage processes, in general. Indeed, if more than one mechanism is involved and these act to a different extent with different impellers, it may well be that the exponent is a function of impeller type. It would also appear probable that the slope should change again when coalescence becomes significant. This change might be expected because, as discussed in detail by Chesters (1991) who considered many coalescence models, coalescence does not have the same functionality in relation to energy dissipation as break-up. This difference has also been discussed in detail by Calabrese et al. (1993).

4. Conclusions

For the first time, equilibrium drop sizes and the rate of approach to that equilibrium size have been reported in which not only a Rushton turbine has been studied but also five other impellers. Altogether, three generic types with two concentrations (1 and 5%) of two dispersed phases, one inviscid and one viscous were studied. Low

power number agitators, whether of the "ultra-high shear" or "high flow" type, produce smaller drop sizes and narrower size distributions than high power number, "high shear" agitators at the same mean energy dissipation rates; and they also do so more rapidly. These findings clearly indicate that there are processing advantages to be gained from choosing a low *Po* impeller when small drops of narrow size distributions are required.

It is difficult to explain these results convincingly. Both the concept of local energy dissipation rates and Reynolds stresses are considered in the paper as the determinants of equilibrium drop sizes but neither matches all the findings. A "circulation time/break-up in the impeller region" model for the rate of approach to equilibrium seems to be satisfactory for the "high flow", low *Po*/high *Fl* impellers but not for the "ultra-high shear", low *Po*/low *Fl* ones. Possibly, as smaller drops are formed by the low *Po* number impellers due to the more intense energy dissipation in the impeller swept volume, these drops, being more rigid, coalesce much less (Calabrese et al., 1993), thereby allowing equilibrium to be reached more rapidly.

It would appear that for further understanding, accurate detailed flow structure characteristics including, for example, local specific energy dissipation rates, need to be measured for a wider range of impellers. However, such measurements are difficult to do if unequivocal values are to be obtained. In addition, more effective coalescence models are required to allow for the possibility that the approach to equilibrium and K_3 in Eq. (5) both depend on drop size as well as the particular liquid–liquid system. Overall, for liquid–liquid systems, more studies are generally needed covering a wider range of impeller types, liquid properties and dispersed phase concentrations.

Notation

b	constant in Eq. (9), dimensionless
d	drop diameter, L
d_{10}	number-length mean diameter, L
d_{32}	surface-volume (Sauter) mean diameter, L
D	impeller diameter, L
Fl	flow number, dimensionless
K_1–K_3	constants in Eqs. (1)–(3) and (5), dimensionless
N	impeller speed, T^{-1}
P	power, $M\,L^2/T^3$
Po	power number, dimensionless
R_{uv}	correlation coefficient in Eq. (13), dimensionless
Re	Reynolds number ($= \rho N D^2/\mu$), dimensionless
t_c	circulation time, T
T	vessel diameter, L
u'	fluctuating velocity in the radial direction, L/T
v'	fluctuating velocity perpendicular to u', L/T
V	vessel volume, L^3
V_{imp}	impeller swept volume, L^3
Vi	viscosity number, $[= (\rho_c/\rho_d)^{0.5} ND\,(\mu_d/\sigma)]$, dimensionless
We	impeller Weber number ($= \rho_c N^2 D^3/\sigma$), dimensionless

Greek letters

ε	local specific energy dissipation rate, L^2/T^3
$\bar{\varepsilon}_T$	mean specific energy dissipation rate, L^2/T^3
μ_c	viscosity of the continuous phase, M/LT
μ_d	viscosity of the dispersed phased, M/LT
Φ	volume fraction of dispersed phase, dimensionless
ρ_c	density of continuous phase, M/L^3
σ	interfacial tension, M/T^2

Subscripts

imp	impeller
max	maximum
r	radial direction
$\mu_d \to 0$	at low viscosity dispersed phase
μ_d	at viscosity of dispersed phase

Acknowledgements

The authors acknowledge the help (i) of the BBSRC who supported the work through a research grant; (ii) of Unilever who provided the sunflower oil and other support, and of the following Ph.D. students (C. C. Man, M. Entwistle, R. Franklin and A. M. Nixon) and an M.Sc. student (S. M. M. Kamal) each of whom provided some of the data used in this paper.

References

Bates, R. L., Fondy, P. L., & Corpstein, R. R. (1963). An examination of some generic parameters of impeller power. *Industrial and Engineering Chemistry, Process Design and Development, 2*, 310–314.

Beck, K. J. (1997). Drop break-up using a saw tooth impeller. *16th NAMF mixing conference*. June, Williamsburg, USA.

Beck, K. J. (1998). *Mechanisms of drop break-up in stirred vessel using a sawtooth impeller*. Ph.D. thesis, School of Mechanical Engineering, Cranfield University, Cranfield, UK.

Bujalski, W., Nienow, A. W., Chatwin, S., & Cooke, M. (1987). Dependency on scale of power numbers of Rushton disc turbines. *Chemical Engineering Science, 42*, 317–326.

Calabrese, R. V. (1997). Liquid–liquid dispersion in low concentration systems: Current needs and understanding. *A.I.Ch.E. 199 annual meeting*, November, Los Angeles, USA, Paper 151a.

Calabrese, R. V., Chang, T. P. K., & Dang, P. T. (1986). Drop break-up in turbulent stirred tank contactors, Part I. Effect of dispersed phase viscosity. *A.I.Ch.E. Journal, 32*, 657–666.

Calabrese, R. V., Pacek, A. W., & Nienow, A. W. (1993). Coalescence of viscous drops in stirred dispersions. *The Institution of Chemical*

Engineers Research Event. Birmingham, January: Institution of Chemical Engineers, Rugby, UK (pp. 642–644).

Calabrese, R. V., & Stoots, C. M. (1989). Flow in the impeller region of a stirred tanks. *Chemical Engineering Progress*, May 43–50.

Chen, H. T., & Middleman, S. (1967). Drop size distribution in agitated liquid–liquid systems. *A.I.Ch.E. Journal*, *13*, 989–995.

Chesters, A. K. (1991). The modelling of coalescence processes in fluid–liquid dispersions: A review of current understanding. *Transactions of the Institute of Chemical Engineering Part A. Chemical Engineering Research and Design*, *69*, 259–270.

Cutter, L. A. (1966). Flow and turbulence in stirred tank. *A.I.Ch.E. Journal*, *12*, 35–44.

Davies, G. A. (1992). Mixing and coalescence phenomena in liquid–liquid systems. In J. D. Thornton, *Science and practice of liquid–liquid extraction, vol. 1* (pp. 245–342). Oxford, U.K: Clarendon Press.

Davies, J. T. (1985). Droplet sizes of emulsions related to turbulent energy dissipation rates. *Chemical Engineering Science*, *40*, 839–842.

Dyster, K. N., Koutsakos, E., Nienow, A. W., & Jaworski, Z. (1993). LDA study of the radial discharge velocities generated by a Rushton Turbines: Newtonian fluids, Re $\geqslant$ 5. *Transactions of the Institute of Chemical Engineers, Part A, Chemical Engineering Research and Design*, *71*, 11–23.

Fondy, P. L., & Bates, R. L. (1963). Agitation of liquid systems requiring a high shear characteristic. *A.I.Ch.E. Journal*, *9*, 338–342.

Godfrey, J. C., Obi, F. I. N., & Reeve, R. N. (1989). Measuring drop size in continuous liquid–liquid mixers. *Chemical Engineering Progress*, *85*, 61–69.

Harnby, N., Edwards, M. F., & Nienow, A. W. (1997). *Mixing in the process industries*. (2nd ed.) (paperback). Oxford: Butterworth-Heinemann.

Hinze, J. O. (1955). Fundamentals of the hydrodynamic mechanism of splitting dispersion process. *A.I.Ch.E. Journal*, *1*, 289–295.

Jaworski, Z., Nienow, A. W., & Dyster, K. N. (1996). An LDA study of the turbulent flow field in a baffled vessel agitated by an axial, down-pumping hydrofoil impeller. *Canadian Journal of Chemical Engineering*, *74*, 3–15.

Lam, A., Sathyagal, A., Kumar, S., & Ramkrishna, D. (1995). On the concept of the maximum stable drop diameter. *A.I.Ch.E. 1995 annual meeting*, November, Miami, USA, Paper 120e.

McManamey, W. J. (1979). Sauter mean and maximum drop diameters of liquid–liquid dispersions in turbulent agitated vessel at low dispersed phase hold-up. *Chemical Engineering Science*, *34*, 432–434.

Nienow, A. W. (1997). On impeller circulation and mixing effectiveness in the turbulent flow regime. *Chemical Engineering Science*, *52*, 2557–2665.

Nienow, A. W. (1998). Hydrodynamics of stirred bioreactors. *Applied Mechanics Reviews*, *51*, 3–32.

Oldshue, J. Y. (1981). *Fluid mixing technology*. New York: McGraw-Hill.

Pacek, A. W., Man, C. C., & Nienow, A. W. (1998). On the Sauter mean diameter and size distributions in turbulent liquid–liquid dispersions in a stirred vessel. *Chemical Engineering Science*, *53*, 2005–2011.

Pacek, A. W., Moore, I. P. T., Nienow, A. W., & Calabrese, R. V. (1994). Video technique for measuring dynamics of liquid–liquid dispersion during phase inversion. *A.I.Ch.E. Journal*, *40*, 1940–1949.

Pacek, A. W., & Nienow, A. W. (1995). Measurement of drop size distribution in concentrated liquid–liquid dispersions: Video and capillary techniques. *Transactions of the Institution of Chemical Engineers, Part A, Chemical Engineering Research and Design*, *73*, Part A, 512–518.

Peters, D. C. (1997). Dynamics of emulsification, In N. Harnby, M. F. Edwards, & A. W. Nienow, *Mixing in the process industries*, (2nd ed., pp. 294–321) (paperback). Oxford: Butterworth-Heinemann's.

Rutherford, K., Lee, K. C., Mahmoudi, S. M. S., & Yianneskis, M. (1996). The influence of Rushton impeller blade and disc thickness on the mixing characteristics of stirred vessels. *Transactions of the Institute of Chemical Engineers, Part A, Chemical Engineering Research and Design*, *74*, 369–379.

Smit, L. (1994). An alternative scale-up procedure for stirred vessels. *Proceedings of Eighth European Mixing Conference*, Cambridge, September: Institution of Chemical Engineers, Rugby, UK (pp. 309–316).

Sprow, F. B. (1967). Distributions of drop sizes produced in turbulent liquid–liquid dispersion. *Chemical Engineering Science*, *22*, 435–444.